

Orbital alignment during cage-exit of open-shell photofragments: F in solid Ar and Kr

K. S. Kizer and V. A. Apkarian

Department of Chemistry, University of California, Irvine, California 92717

(Received 12 April 1995; accepted 19 June 1995)

The statistical theory for sudden cage-exit [J. Zoval and V. A. Apkarian, *J. Phys. Chem.* **98**, 7945 (1994)] is extended to orbitally degenerate photofragments, specifically treating the case of F atoms in solid Ar and Kr. It is shown that the experimental energy-dependent quantum yields of photodissociation of F₂ are only compatible with the *p* hole on the F atom being completely aligned parallel to the cage wall during the sudden exit. Although relative quantum yields and energy thresholds are well predicted, the calculated absolute quantum yields are a factor of ~ 2 smaller than the experimental values. © 1995 American Institute of Physics.

I. INTRODUCTION

The many-body dynamics of open-shell fragments, with orbital degeneracy ($1 > 1$), cannot be described by a single potential-energy surface. In effect, the Born–Oppenheimer separation between electronic and nuclear degrees of freedom breaks down, and it is necessary to consider the coupled electronic nuclear motions in describing processes relevant to chemistry. The cage-exit dynamics of an F atom in rare gas solids represents the simplest possible case to consider such an effect. Given the small spin–orbit splitting in F atoms, as compared to photodissociation energies, the multiplicity of electronic surfaces can be reduced to a description of the alignment of the *p*-hole relative to the atomic coordinates. In this paper, we consider the effect of orbital alignment on photodissociation quantum yields, and conclude that the experimental energy dependent dissociation probabilities are only consistent with full alignment. The analysis is based on the statistical treatment of sudden cage-exit probabilities, which was recently advanced for the treatment of photodissociation of hydrides.¹

Dissociative excitation of small molecules isolated in rare gas solids, at excess energies of several eV ($E_{\text{excess}} = \hbar\omega - D_0$), leads to a wide range of behaviors—from complete caging to near unit dissociation quantum yields. Among examples which have been reported to show complete caging are CH₃I (Ref. 2), ICl (Ref. 3), Cl₂ (Ref. 4), Br₂ (Ref. 5), I₂ (Ref. 6), ICN (Ref. 7), and O₂ (Ref. 8). While “complete caging” is seldom quantified, upper limits of photodissociation quantum yields, Φ , have been established in a few of these cases. As an example, in the case of Cl₂ isolated in Ar, at an excess energy of 1.5 eV, $\Phi < 10^{-6.9}$. In contrast, facile photodissociation accompanied by permanent separation of photofragments is observed in cases where the photoproduct is a “small” atom, i.e., where the photoproduct-host potential has a short interaction range. Photodissociation of hydrides and, in particular, H₂O (Ref. 10) and H₂S (Refs. 1 and 11) to produce interstitial H atoms, photodissociation of F₂, (Refs. 12 and 13), photodissociation of N₂O (Refs. 8 and 14) and O₃ (Ref. 15) to produce atomic oxygen, and OCS to produce atomic sulfur, (Ref. 16), are among the examples that belong to the second category. Among these, the most facile photodissociation is observed for F₂ which, in

crystalline Ar and Kr hosts, yield $\Phi \sim 1$ at $E_{\text{excess}} \geq 2.4$ eV.¹² Photodissociation products are generally open-shell fragments and, therefore, with the exception of *S* states, their dynamics will be determined by forces acting on anisotropic charge distributions. In the examples cited, we note that at comparable excess energies, while the photodissociation quantum yield of O₂ is negligible, N₂O and O₃ dissociate with near unit probability in a variety of hosts. This difference can be ascribed to the nascent electronic state of the O atom: O(³*P*) in the case of photodissociation of O₂, and O(¹*D*) in the cases of O₃ and N₂O. The dramatic difference between potential energy surfaces of O(¹*D*) and O(³*P*) in rare gas hosts has already been discussed.¹⁷ First, in rare gas solids O(¹*D*) is much smaller than O(³*P*). Based on pair potential minima, which is a consideration useful for establishing the stability of final states, O(¹*D*) is more than 1 Å smaller than O(³*P*).¹⁸ Based on repulsive walls of pair potentials, which is a consideration crucial to the cage exit dynamics, at $E_{\text{excess}} \sim 2$ eV, on its ¹ Σ surface O(¹*D*) is ~ 0.5 Å smaller than O(³*P*) on its ³ Π surface.¹⁸ Moreover, consideration of global surfaces shows that the minimum energy paths between two stationary points in the lattice are quite different for the two electronic surfaces.¹⁷ Similar considerations would seem to apply for sulfur atoms. The observation of the S+H₂ channel in the photodissociation of H₂S has been attributed to production of S(¹*D*).¹¹ The photodissociation of OCS, which proceeds via S(¹*D*) leads to permanent production of sulfur atoms, while in the case of CS₂ which proceeds via S(³*P*), the permanent dissociation is dominated by the S₂ channel (presumably C+S₂).¹⁶ This strong dependence on the particular electronic state of a given atom is not too surprising. Nevertheless, few systems have been rigorously treated with respect to the coupling between electronic and nuclear degrees of freedom.

The first molecular dynamics simulations using multiple electronic surfaces, allowing for nonadiabatic dynamics, was presented by Gersonde and Gabriel in their treatments of HCl and Cl₂ photodissociation in rare gas solids.¹⁹ Effects of nonadiabaticity on thermal motions of F atoms isolated in Ar, and in simulations of the Ar₂F radiative dissociation were discussed more recently.²⁰ In these treatments, although pair potentials are used, the assumption of pairwise additivity is no longer made: the interaction Hamiltonians are limited to

the $l=1$ basis set on the halogen atom, and expanded in a diatomics-in-molecules (DIM) sense using the known gas phase pair potentials with the neglect of spin-orbit interactions. The same approach, with the inclusion of spin-orbit terms, has been successful in reproducing the experimental spectra of I atoms trapped in solid Kr and Xe in the adiabatic following limit.²¹ This, and simulations of site specific emission spectra of $O(^1S) \rightarrow O(^1D)$ transitions in the same solids,¹⁷ have shown that with only minor modifications to pair parameters the energetics of open-shell atoms at stable trapping sites are adequately treated. A similar gauge of accuracy does not yet exist for treatments of dynamics where the requirements on assumed potentials are more stringent, since entire surfaces including nonstationary points, such as saddle points and potential barriers are required. Photodissociation experiments can serve as a probe of such surfaces, and can be used as models to develop a better understanding of the relation between many-body and pair interactions.

The photodissociation of F_2 has been studied experimentally in free standing rare gas crystals, providing data on quantum yields of dissociation as a function of excess energy.^{12,13} It has also been shown that at 4.5 K, dissociation probabilities are twice that at 12 K.¹³ This has been taken as evidence of direct dissociation via cones of cage exit; at low temperatures the molecules orient along the exit cone, while at higher temperatures due to nearly free rotation of the molecule, the orientational bias is lost. Beside facile dissociation long-range mobility of F atoms has been demonstrated and quantified.¹² The system has also been studied by molecular dynamics simulations.^{20,22,23} The first such classical simulation relied on a pairwise additive potential, using the lowest energy RgF(X) pair potential.²² The simulations were in good *qualitative* agreement with experiments, predicted the temperature dependence subsequently observed in experiments, and reproduced the observed long-range mobility of atoms subsequent to dissociation. Quantitative agreement with observed quantum yields was obtained when the results of simulations carried separately on the RgF(X) and RgF(A) pair potentials were averaged.²³ Despite the *ad hoc* nature of this treatment, it clearly indicated that a strictly classical, single surface simulation is inadequate for describing the many-body dynamics of systems containing open shell fragments.

The large photodissociation quantum yields of F_2 , the observed control of exit on molecule-lattice prealignment, and the approximate classical simulations of this system all indicate that the cage exit of F atoms is dominated by *sudden exit* dynamics: exit over the cage potential barriers, without significant distortion of the lattice. A statistical model valid in this limit, and consistent with the main experimental findings, was recently presented for the analysis of photodissociation probabilities of hydrides in rare gas solids.¹ In essence, the model treats photodissociation as an experiment in *scattering from within* the solid. Cage-exit probabilities are then determined by the molecular orientation relative to the cage windows and the energy dependent window cross sections which are properly weighted by distributions arising from lattice fluctuations. In the case of orbitally degenerate open shell fragments, it is necessary to consider the depen-

dence of potential energy surfaces on orbital alignment as well. We construct such a model for F atoms in solid Ar and Kr, and based on the experimental energy dependent quantum yields of dissociation of F_2 , dwell on the implied extent of orbital alignment during the sudden dynamics of photodissociation at excess energies of several eV. Despite the simplifying assumptions made in the statistical treatment, firm conclusions can be reached about this issue.

II. THE STATISTICAL PROBABILITIES

Permanent photodissociation of a diatomic in a solid is contingent upon separation of the photoproducts by cage-exit of at least one of the fragments. For a substitutionally trapped parent molecule, in a crystalline fcc lattice, for dissociation, minimally, the ejection of a photofragment to the nearest interstitial octahedral site is required. This is illustrated in Fig. 1. The minimum energy path to such an interstitial site involves passage through one of the faces of the octahedron, which is constructed by three mutual nearest neighbor atoms of the host lattice [Fig. 1(b)]. This is also the plane that contains the potential barrier along the minimum energy path, and constitutes the cage wall through which the atom must exit. The potential-energy surfaces in this plane are determined by the instantaneous positions of the lattice points, and the interaction potential between the projectile, F in the present, and the rare gas host atoms. Explicit account of the dependence of this interaction on the electronic coordinate, r , of the F atom is necessary. The potential energy contours for perpendicular and parallel alignment of the orbital as it approaches this plane are illustrated in Figs. 1(c) and 1(d).

Limiting ourselves to the three rare gas atoms that constitute a cage wall, with coordinates R_i relative to the F atom position, and ignoring spin-orbit terms, the electrostatic interaction

$$H_{\text{int}} = V_{\text{F-Rg}}(r; R_1, R_2, R_3) \quad (1)$$

can be most generally evaluated by expanding it in Legendre polynomials. In the limited p_i ($i=x, y, z$) basis set on the F atom, only two terms contribute to this expansion:

$$H_{\text{int}} = \sum_{i=1}^3 [V_0(R_i) + V_2(R_i)P_2(\vec{R}_i \cdot \vec{r})] \quad (2)$$

in which V_0 and V_2 refer to the isotropic and anisotropic components of the F-Rg pair potentials.²¹ The interaction potentials can then be obtained as expectation values over the electronic distribution, by diagonalizing the 3×3 Hamiltonian with elements

$$V_{ij} = \langle p_j | H_{\text{int}} | p_i \rangle. \quad (3)$$

In the D_{3h} symmetry of attack, two eigenvalues arise: one for perpendicular alignment of the p -hole relative to the plane of the wall, and one for parallel alignment. We refer to these surfaces as V_{\perp} and V_{\parallel} . At lower symmetries than D_{3h} , eigenvalues of the parallel alignment will further split; we will retain the lower of these values throughout our discussion. The equipotentials for these two alignments, for an F atom at the wall in solid Kr, are also illustrated in Figs. 1(c)

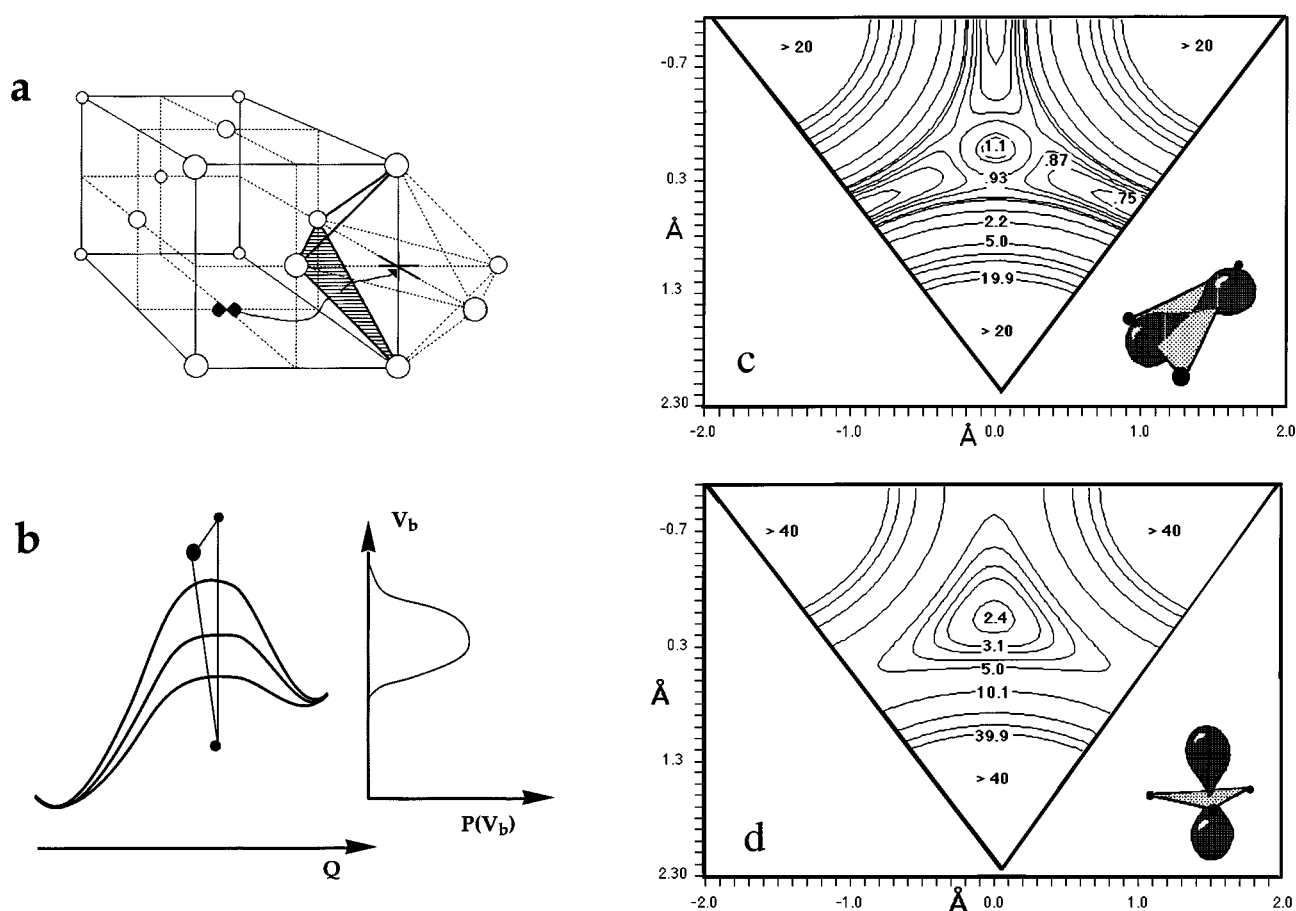


FIG. 1. (a) Reaction coordinate: The rare gas unit cell is shown with a substitutionally trapped F_2 molecule. The arrow shows the minimum energy path of dissociation, which passes through a potential barrier occurring in the plane of the octahedron constructed by the three mutual nearest-neighbor rare gas atoms. (b) The potential barrier along the reaction coordinate is subject to a distribution due to the distribution in the positions of host atoms effected by thermal and zero-point fluctuations. The potential-energy surfaces on the dividing plane are shown as equipotentials for (c) parallel alignment of the p hole with the plane; (d) perpendicular alignment of the p hole with the plane. The data are for F-Kr, for the equilibrium structure of the lattice.

and 1(d). The required pair potential inputs, V_0 and V_2 , are taken from Aquilanti *et al.* and are based on gas phase scattering data.²⁴ The evaluation in Fig. 1 is for the equilibrium geometry of the lattice.

The differences between V_{\perp} and V_{\parallel} surfaces deserve some consideration. The minima of these surfaces constitute the potential barriers, V_b , along the minimum energy path to be traversed by the exiting atom. For the equilibrium geometry of the lattice, the barrier heights are $V_{b,\perp}=1.6$ eV and $V_{b,\parallel}=0.6$ eV in Ar, and $V_{b,\perp}=2.4$ eV and $V_{b,\parallel}=0.7$ eV in Kr. This difference in barrier heights is due to the anisotropy of repulsive walls of potentials which are amplified by the cramped threefold coordination. The potential-energy surface topologies are quite different for the two alignments. In the case of perpendicular approach, where the electron density is maximized in the plane of the wall, the potential-energy barrier occurs in the middle of the triangle. Here, in terms of the nearest-neighbor distance, d (side of triangle), the barrier height is given as

$$V_{b,\perp}=3V_{II}(d\sqrt{3}/6). \quad (4)$$

In the case of parallel alignment, the minimum occurs at the insertion site between a pair of nearest neighbors. In the insertion site, the barrier height is given as

$$V_{b,\parallel}=2V_{\Sigma}(d/2)+V_{II}(d\sqrt{3}/4). \quad (5)$$

Thus the cage-exit barrier heights can be directly estimated from the known pair potentials, using Eqs. (4) and (5). We note that these evaluations are approximate, since they do not include summations over all lattice points. However, this approximation is not too serious, since we are concerned with differences in potentials between trapping sites and barrier heights, and the infinite summation is present in both. The relevant surfaces are dominated by differences in the short range part of interactions.

Under the assumption of a random initial orientation of the molecule relative to the cage wall, for a fixed geometry of the wall, and for a particular alignment of the p hole, the probability of sudden exit of an atom with energy E is equated to the transmission coefficient: $\kappa(E, V_b)=\text{window area/wall area}$. The area of the window is defined by the equipotential at E , while the area of the wall is that of the triangular face of the octahedron. These quantities are clearly dependent on the wall configurations, or equivalently on the distribution of positions that arise from thermal and zero-point fluctuations of the lattice. Taking this distribution into account, the single trial exit probability is given as

$$\phi(E) = \int_{V_b=0}^{V_b=E} \kappa(E, V_b) P(V_b; \{R_i\}) dV_b \quad (6)$$

which is the main result of the statistical model for sudden cage exit.¹ Here, we explicitly indicate the fact that V_b is a function of the positions of the wall atoms and, hence, the distribution in barrier heights is strictly due to the distribution in lattice positions. The latter is taken into account by considering the symmetric vibrations of the wall, as the Rg_3 harmonic quantum oscillator in equilibrium with its thermal bath. In the limited amplitude range of such vibrations, V_b can be expressed as an exponential function of the vibrational coordinate, and hence distributions in position can be analytically inverted to a distribution in barrier heights. The calculated and exponential fits to $V_{b,\perp}$ and $V_{b,\parallel}$ are shown in the insets in Fig. 2, as a function of the internal coordinate of the F- Rg_3 complex, q , which is defined as the distance from the center to apex of the triangle. The resulting barrier height distributions can be expressed analytically as

$$P(V_b, T) = \frac{\rho(q, T)}{dV_b/dq}, \quad (7a)$$

$$P(V_b, T) = \frac{1}{(\pi)\xi\beta V_b} \exp\left\{-\left[\frac{1}{\beta} \ln\left(\frac{V}{3A}\right) + q_0\right]^2 / \xi^2\right\}, \quad (7b)$$

and are shown in Fig. 2, and the parameters are collected in Table I. $\rho(q, t)$ is the Gaussian distribution of positions, ξ is the width of the distribution of positions, q_0 is the equilibrium distance of rare gas atoms as measured from the center of the triangle of the rare gas atom,¹ and A and β are the preexponential and exponential values from the fit of $V_{b,\perp}$ and $V_{b,\parallel}$ (see insets to Fig. 2). The distributions, although evaluated at 15 K, are quite broad due to the highly repulsive nature of interactions in the plane of the wall (shaded area in insets to Fig. 2). The distributions for different alignments are energetically distinct, and should therefore, be distinguishable experimentally.

The transmission coefficient, κ in Eq. (6), can also be expressed analytically. In Fig. 3 we show κ for the full range of amplitudes of the vibrational fluctuations of Rg_3 , for both perpendicular and parallel alignments. When plotted vs a reduced energy abscissa, $E^* = (E - V_b)/V_b$, it can be seen that, to a good approximation, the transmission coefficients can be expressed as a single analytical function, independent of the vibrational amplitude of the Rg_3 . A different function is required for each alignment. The following forms were used for fitting the transmission coefficients:

$$\kappa(E, V_{b,\parallel}) = a + be^{-E^*/c} + de^{-E^*/f}, \quad (8a)$$

$$\kappa(E, V_{b,\perp}) = a + be^{-E^*/c}, \quad (8b)$$

the parameters for these fits are also collected in Table I. These fits are made for $E^* = 0-5$, which corresponds to total excess energies up to 4 eV, for the parallel case, and 15 eV for the perpendicular case and, therefore, valid for any prac-

tical photodissociation experiment. Note, κ reaches a value of ~ 0.3 , therefore, in a single trial, exit probabilities cannot exceed this value.

Given analytical expressions for $\kappa(E, V_b)$ and $P(V_b)$, the cage exit probabilities can be evaluated for each alignment, the results are shown in Fig. 4. Expressions for multiple trial exit probabilities, which are quite significant for the case of H atoms, have been given and discussed. For binary collisions with stationary host atoms, the fractional energy loss per collision averaged over scattering angles is given as $\Delta E/E = 2mM/(m+M)^2$. For F atoms in Ar and Kr, this predicts 44% and 30% energy loss per collision, respectively. Thus, the atom can only have several attempts at cage-exit before its energy drops below the threshold of the barrier height distribution. The validity of this kinematics could be more rigorously tested by molecular dynamics simulations, the existing simulations show that indeed cage exit is limited to the first few collisions with the lattice.^{22,23} Defining $\gamma = 1 - \Delta E/E$, the multiple trial exit probabilities can be computed rather directly as¹

$$\Phi(E) = \sum_{j=1}^n [\Phi_j(E)], \quad (9a)$$

$$\Phi_j(E) = \left(1 - \sum_i^{n-1} \Phi_i(E)\right) \Phi(\gamma^{n-1}, E) - \frac{1}{8} \Phi(\gamma^n, E), \quad (9b)$$

where n is the number of trials, $n \leq 3$. The predicted quantum yields of cage-exit of Eq. (9), are also shown in Fig. 4. These probabilities show a steeper energy dependence near threshold, and reach a saturation limit $\sim 50\%$ larger than the single trial probabilities. Note that the efficient energy loss in this system also implies that the relative molecule-window orientations will have a significant effect. If initially the F atom is locked into an orientation that results in a direct hit with one of the cage atoms, such that the initial trial is doomed to fail, then cage-exit probabilities will be reduced by $\sim 50\%$. If tightly oriented toward a window, then a transmission coefficient larger than statistical will be in effect. The experimental temperature dependent studies of F_2 dissociation have already shown this strong orientational effect.¹³ At $T > 12$ K, the molecule is presumed to be a nearly free rotor, and therefore no orientational bias on dynamics is to be expected.

Quite clearly, the sudden exit model will be limited in its applications to small atoms, or systems with large κ at low excess energy. In fact, consideration of the energetics makes it obvious that already in the case of Cl/Xe the model will break down. To see this we proceed in the same fashion as earlier to generate $P(V_b)$ for Cl cage-exit as would be expected in the case of Cl_2 or ICl dissociation. To this end, we rely on the anisotropic pair potentials of Acquilanti *et al.*²⁵ Figure 5 shows $P(V_b)$ to have a threshold near 6.5 eV and, in fact, for the perpendicular approach V_b is of order 20 eV. At these excess energies, a projectile may “push” the cage atoms, opening its own window. This system has been studied both experimentally, and by molecular dynamics simulations.^{26,27} Although the simulations are carried out on a single surface, the experimentally observed energetic threshold, which is also in agreement with the oriented at-

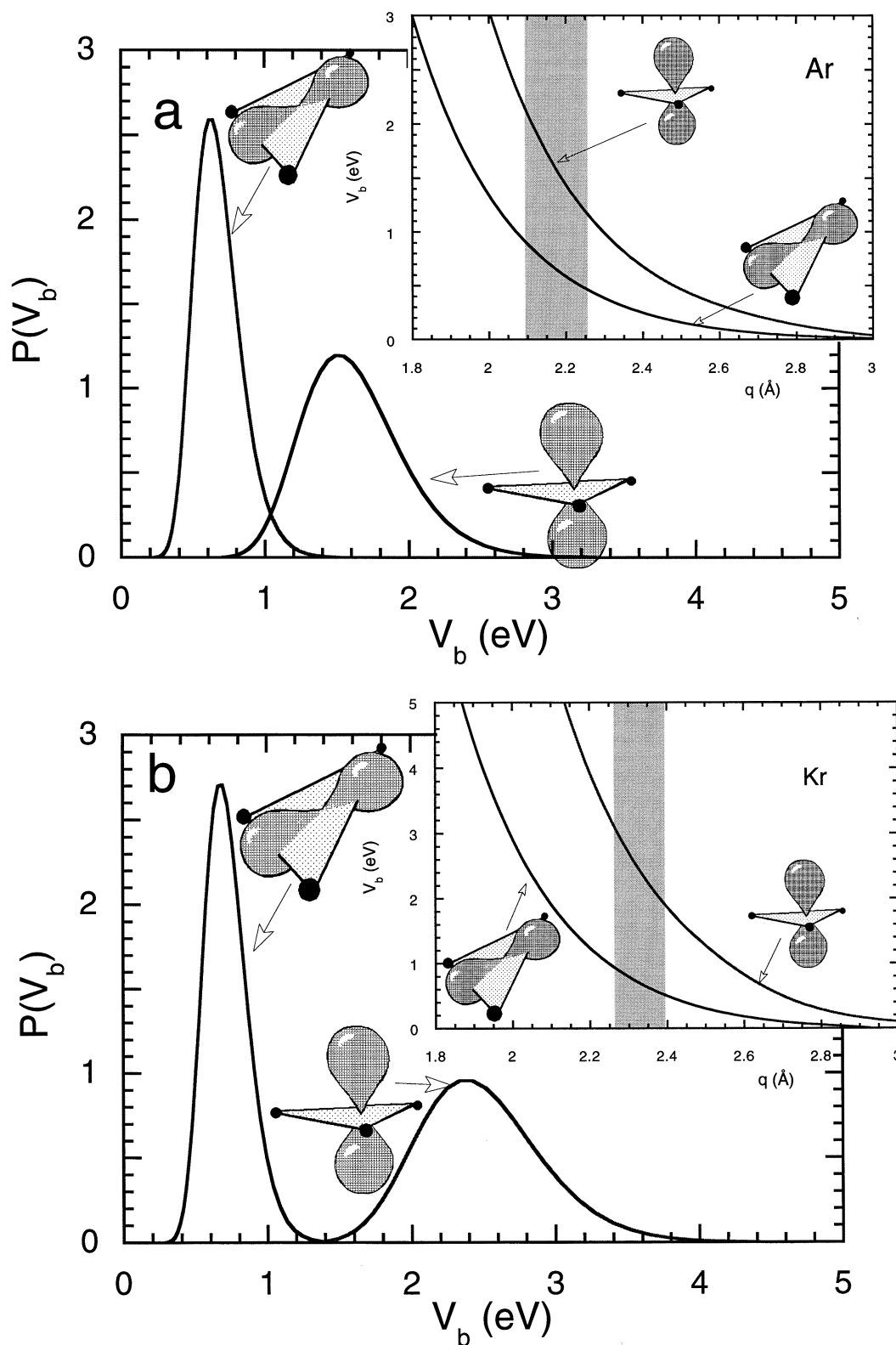


FIG. 2. Barrier height distributions for parallel and perpendicular alignment of the p hole. (a) F in Ar; (b) F in Kr. For each case in the inset the calculated potentials for V_{\perp} and V_{\parallel} are shown [Eqs. (4) and (5) in text] plotted vs q (center to apex of the triangle). The shaded regions correspond to the thermally accessible, relevant amplitudes of q which is used in the calculation of distributions.

tack, of ~ 6.5 eV is reproduced. The trajectories at these and higher energies show significant dislodging of the host atoms, implying exit over potential barriers that are “carved out” by the exiting atom.

III. DISCUSSION

The statistical treatment presented is for cage-exit of F atoms, as a function of energy. The relevant experiments are

TABLE I. Curve fit parameters.

		Ar	Kr
V_b , parallel ^a	A (eV)	5486.8	32616
	β (\AA^{-1})	4.1552	4.6196
V_b , perpendicular ^a	A (eV)	5663.2	14634
	β (\AA^{-1})	3.7621	3.7362
$\rho(q, T)$ ^b	q_0 (\AA)	2.174	2.327
	ζ (\AA)	0.0806	0.0651
$K(E, V_b)$, parallel ^c	a	0.2485	0.5684
	b	-0.2497	-0.5596
	c	3.2631	3.6896
$K(E, V_b)$, perpendicular ^c	a	0.4149	0.6414
	b	0.2304	0.3890
	c	9.3387	6.8619
	d	-0.1914	-0.2507
	f	0.5440	0.2798

^aParameters of exponential fits of V_b used in Eq. (7a) of text.

^bParameters of distribution of position, used in Eq. (7b) of text, taken from Ref. 1.

^cParameters of curve fit to transmission probability in Eqs. (8a) and (8b) of text.

conducted on F_2 isolated in free standing crystals of Ar and Kr, as a function of excitation energy. We proceed with the assumption that the initial excess energy is equally divided between the two F atoms, and ignore possibilities of energy exchange between the two photofragments. Accordingly, we divide the experimental excess energy by two in making

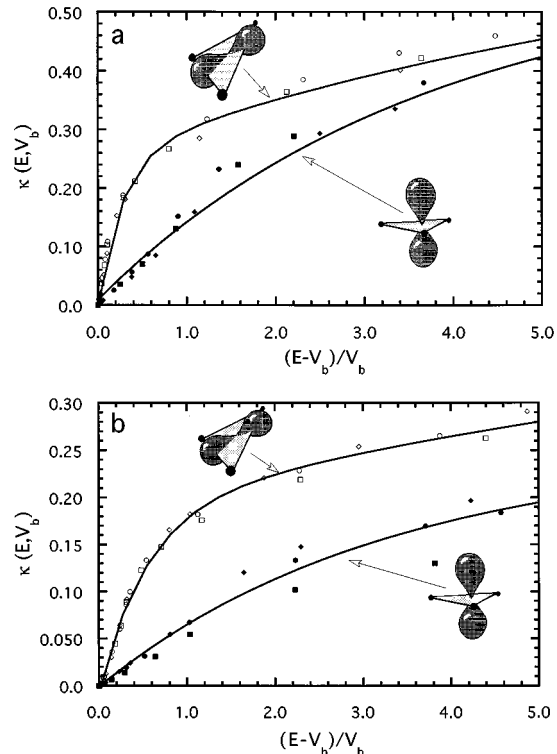


FIG. 3. Transmission probability, $\kappa(E, V_b)$, as a function of reduced energy, $E^* = (E - V_b)/V_b$, for parallel and perpendicular alignment of the p hole. (a) F in Ar where the nearest-neighbor distances of the Ar atoms are square = 3.9 Å; circle = 3.8 Å; diamond = 3.6 Å. (b) F in Kr where the nearest-neighbor distances of the Kr atoms are square = 4.1 Å; circle = 4.0 Å; diamond = 3.9 Å. For each case the analytical fit to κ [Eqs. 8(a) and 8(b) in text] are also shown.

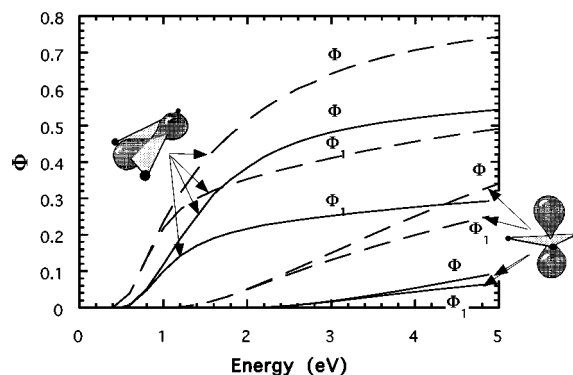


FIG. 4. Quantum yields of F atom exit, in Kr (solid lines) and Ar (dashed lines) at 15 K vs excess energy. The single trial probabilities, Φ_1 , and the multiple trial probabilities, Φ , are shown for each alignment case.

comparisons with the present predictions. The experimental data^{22,23} are shown in Fig. 6, together with the theoretical predictions. Two linear ordinates are used in this presentation, the right ordinate is the experimental quantum yield while the left ordinate is for the theory. They are scaled by approximately matching the plateaus. It can be seen in Fig. 6 that, with the exception of the absolute values of quantum yields, the data are reasonably well reproduced by the theoretical predictions under the assumption that the atoms are fully aligned parallel to the cage wall during exit. Both the observed dissociation thresholds, and the energy dependence of quantum yields are well reproduced. It is noteworthy that in the case of Kr, the experimental quantum yields reach unit probability prior to opening of the perpendicular alignment channel. This strongly suggests that independent of initial orientation of the hole, the torque exerted by the anisotropic F-Rg potential is sufficient to realign the hole by the time it reaches the cage wall. If there were any contributions from perpendicular alignment, then we would not observe unit quantum yields at these energies. Since the molecule-cage orientations are randomized by the nearly free rotations of F_2 , photodissociation will then create the F atom on either of the perpendicular or parallel adiabatic surfaces initially. Complete alignment therefore implies that nonadiabatic switching of surfaces occurs prior to reaching the cage-exit barrier.

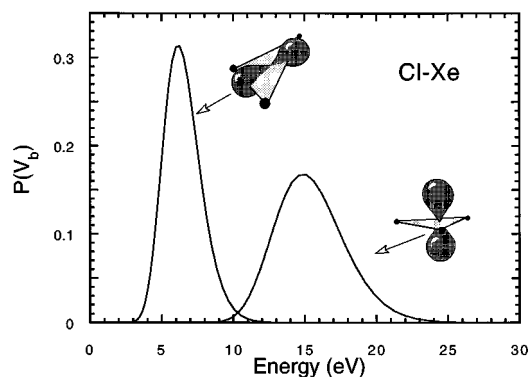


FIG. 5. The normalized barrier height distributions versus excess energy for Cl atoms in Sid Xe (at 15 K) for parallel and perpendicular alignment.

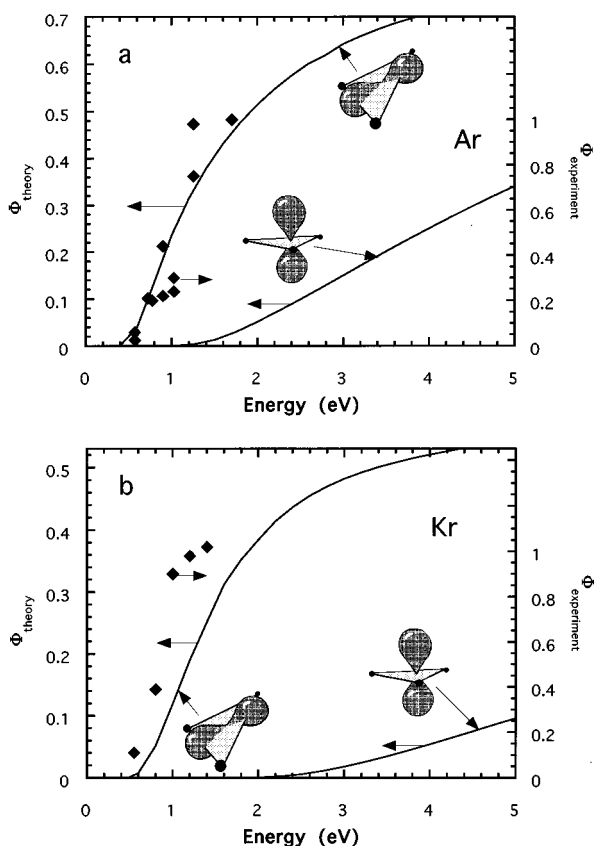


FIG. 6. Comparison of the theoretically predicted quantum yields, Φ_{theory} , (the left-hand ordinate) with the experimental quantum yields, Φ_{expt} (the right-hand ordinate). The plateaus of Φ_{theory} and Φ_{expt} are approximately matched, showing a factor of 2 difference in the ordinates. The Φ_{theory} of photodissociation for both parallel and perpendicular alignment are also indicated: (a) F in Ar; (b) F in Kr.

There are several possible origins of the discrepancy between predicted and observed absolute quantum yields. The most obvious is that the description of potentials, based strictly on pair interactions and limited to the covalent basis set, is a poor approximation in the cage barrier region. We expect that in these tight geometries a significant admixture from Rg^+F^- charge transfer configurations will contribute to the interactions. This would lead to reduction of interaction potentials, and to enhancement of transmission coefficients κ , leading to exit probabilities larger than predicted. In treating charge transfer states of halogens in rare gas matrices, the diatomics-in-molecules- (DIM) type surfaces have been constructed previously.²⁸ It would be quite informative to test the results of such an expanded basis set on the predictions of the present model.

Assuming that the potential surfaces are of acceptable validity, and not withstanding the obvious approximations made, the discrepancy between experiment and statistical model would be indicative of dynamical biases. Preferential orientation of the molecular axis toward the exit window would lead to larger exit probabilities than the purely statistical assumption. The temperature experiments indicate that at 15 K it is safe to assume that F_2 is orientationally isotropic. A more significant consideration is that a strictly sudden limit is not valid in the present case. In contrast with H

atoms, in the case of F in Ar and in Kr, significant momentum transfer occurs during the collision with the cage atoms. This, in effect, would lead to opening of windows where there was none in the thermal distribution of lattice configurations, leading to transmission coefficients larger than predicted by the sudden limit. Finally, the assumption of isolated binary collisions in calculating multiple trial probabilities is somewhat suspect. We may expect deviations from this to lead to a significantly larger effective mass of the host, therefore less efficient energy loss of the projectile than assumed. The latter would lead to an increase in the number of trials and, therefore, to larger probabilities than computed. The fact that each of these contributions—the potentials, orientational bias, and dynamical contributions to window cross sections—will all lead to larger quantum yields than predicted, implies that none of these corrections alone would change the general picture, that the orbital is fully aligned during cage-exit.

It is possible to surmise that the aforementioned conclusions are not unique to F atoms. In fact, given the similarity of experimental observations in the case of $\text{O}(^1D)$ cage-exit, large quantum yields and a strong temperature dependence,^{14,15} we expect the present model modified to treat the two-hole atom should be valid. The model is, however, clearly inadequate in the case of larger atoms. Already in the case of Cl, although energetic thresholds can be predicted, transmission coefficients are too small to rationalize observed experimental behavior. In cases where excess energies of many eV are required to reach dissociation thresholds, the window opening by momentum transfer will play a crucial role in dissociation probabilities.

As already mentioned, classical molecular dynamics simulations using single potential energy surfaces have in the case of F_2 and Cl_2 dissociation yielded nearly quantitative agreement with experiments.^{22,23,27} The reason for this success seems now understandable. The initial simulations assumed a pairwise additive $\text{RgF}(X)$ surface, effectively assuming a Σ pair interaction.²² Note, this is not realizable even if one were to assume fully adiabatic dynamics. At the transition state, in the three atom plane, this yields three Σ interactions, instead of the proper eigenstate, which for the minimum yields Eq. (5) (two Σ interactions with the nearest atoms and a Π contribution for the furthest atom). Not surprisingly, the simulations yielded larger probabilities and lower threshold energies than observed. The subsequent improvement of simulation predictions is somewhat more *ad hoc*.²³ Simulations were separately carried out on the $\text{RgF}(A)$ surface, which is Π in character. At the barrier, this would be exactly that of Eq. (4), i.e., the high energy eigenstate of the system. Clearly, dissociation probabilities are nearly zero for this case in the energy range of interest (0.5–2.5 eV). By averaging the results of these independent simulations, neither of which individually represents dynamics over a realizable surface, brings about the quantitative agreement between experiment and simulation.²³ The quantitative agreement must be regarded as fortuitous, since the simulations are for qualitatively different physics. The methodologies for carrying out multiple surface dynamics without as-

sumptions of adiabaticity exist, and would be quite useful if applied to this model system.^{19,20}

IV. CONCLUSIONS

We conclude that the photodissociation of F₂ is dominated by F atom exit over potential energy barriers provided by the cage walls. A process dominated by sudden exit dynamics as far as the nuclear motions are concerned. Despite the sudden nature of this cage exit, at excess energies of several eV, the torque exerted by the anisotropic atomic potentials is sufficient to fully align the *p* hole on the F atom during the $\sim 10^{-13}$ s required to reach the cage wall. Since the initial orientations created by the photodissociation process are random, we must also infer efficient nonadiabatic switching between the perpendicular and parallel adiabatic potential energy surfaces. This model system could be further exploited. Ultrafast pump-probe experiments with polarization selection can, in principle, provide a direct observation of orbital reorientation, as outlined in recent studies of caging.²⁹ Simulations that treat coupled electronic nuclear motions on an equal par, are required for the analysis of such data.

The above conclusions are based on the statistical theory of *sudden cage exit* which, although approximate, reproduces the observed relative quantum yields of dissociation and seems to account for the main features of the underlying dynamics. The present model is limited to the case of small photofragments which show large quantum yields of dissociation at low excess energies. Comparison of such models to detailed observations can serve as the basis of establishing dynamical biases, and the development of models that go beyond the sudden limit.

ACKNOWLEDGMENT

This research was supported under a grant from the U.S. Air Force Office of Scientific Research AFOSRF49620-1-0251.

¹J. Zoval and V. A. Apkarian, *J. Phys. Chem.* **98**, 7945 (1994).

²L. E. Brus and V. E. Bondybey, *J. Chem. Phys.* **65**, 71 (1976); *Chem. Phys. Lett.* **36**, 252, (1975).

³V. E. Bondybey and L. E. Brus, *J. Chem. Phys.* **65**, 620 (1975); **64**, 3724 (1976).

⁴V. E. Bondybey and C. Fletcher, *J. Chem. Phys.* **64**, 3615 (1976).

⁵V. E. Bondybey, S. S. Bearder, and C. Fletcher, *J. Chem. Phys.* **64**, 5243 (1976); P. Beeken, M. Mandich, and G. Flynn, *J. Chem. Phys.* **76**, 5995 (1982); M. Mandich, P. Beeken, and G. Flynn, *J. Chem. Phys.* **77**, 702 (1982).

⁶P. B. Beeken, E. A. Hanson, and G. W. Flynn, *J. Chem. Phys.* **78**, 5892, (1983); R. Zadoyan, Z. Li, C. C. Martens, P. Ashjian, and V. A. Apkarian, *Chem. Phys. Lett.* **218**, 504 (1994); R. Zadoyan, Z. Li, C. C. Martens, and V. A. Apkarian, *J. Chem. Phys.* **101**, 6648 (1994).

⁷R. Fraenkel and Y. Haas, *Chem. Phys. Lett.* **214**, 234 (1993); **226**, 610 (1993).

⁸W. G. Lawrence and V. A. Apkarian, *J. Chem. Phys.* **97**, 2229 (1992); A. V. Danilychev and V. A. Apkarian, *ibid.* **99**, 8617 (1993).

⁹M. E. Fajardo, R. Whitnall, J. Feld, F. Okada, W. Lawrence, L. Wiedeman, and V. A. Apkarian, *Laser Chem.* **9**, 1 (1988).

¹⁰R. Schrieffer, M. Chergui, and N. Schwentner, *J. Phys. Chem. Phys.* **95**, 6124 (1991); R. Schrieffer, M. Chergui, O. Unal, V. Stepanenko, and N. Schwentner, *J. Chem. Phys.* **91**, 4128 (1989); **93**, 3245 (1990).

¹¹J. Zoval, D. Imre, P. Ashjian, and V. A. Apkarian, *Chem. Phys. Lett.* **197**, 549 (1992).

¹²H. Kunttu, J. Feld, R. Alimi, and V. A. Apkarian, *J. Chem. Phys.* **92**, 4856, (1990); J. Feld, H. Kunttu, and V. A. Apkarian, *ibid.* **93**, 1009 (1990); H. Kunttu, E. Sekreta, and V. A. Apkarian, *ibid.* **94**, 7819, (1991).

¹³H. Kunttu and V. A. Apkarian, *Chem. Phys. Lett.* **171**, 423 (1990).

¹⁴E. T. Ryan and E. Weitz, *Chem. Phys.* **189**, 293 (1994).

¹⁵A. V. Benderskii and C. A. Wight, *Chem. Phys.* **189**, 307 (1994); *J. Chem. Phys.* **101**, 292 (1994).

¹⁶S. Tanaka, H. Kajihara, S. Koda, and V. A. Apkarian, *Chem. Phys. Lett.* **233**, 555 (1995).

¹⁷A. V. Danilychev and V. A. Apkarian, *J. Chem. Phys.* **100**, 5556 (1994).

¹⁸T. H. Dunning, Jr. and P. J. Hay, *J. Chem. Phys.* **66**, 3767 (1977); **74**, 3718 (1981).

¹⁹I. H. Gersonde and H. Gabriel, *J. Chem. Phys.* **98**, 2094 (1993); I. H. Gersonde, S. Henning, and H. Gabriel, *ibid.* **101**, 9558 (1994).

²⁰A. Krylov, R. B. Gerber, and V. A. Apkarian, *Chem. Phys.* **189**, 261 (1994).

²¹W. G. Lawrence and V. A. Apkarian, *J. Chem. Phys.* **101**, 1820, (1994).

²²R. Alimi, R. B. Gerber, and V. A. Apkarian, *J. Chem. Phys.* **92**, 3551 (1990).

²³R. Alimi, R. B. Gerber, and V. A. Apkarian, *Phys. Rev. Lett.* **66**, 1295 (1991).

²⁴V. Aquilanti, E. Luzzatti, F. Pirani, and G. G. Volpi, *J. Chem. Phys.* **89**, 6165 (1988).

²⁵V. Aquilanti, D. Cappalletti, V. Lorent, E. Luzzatti, and F. Pirani, *Chem. Phys. Lett.* **192**, 153 (1992).

²⁶J. G. McCaffrey, H. Kunz, and N. Schwentner, *J. Chem. Phys.* **96**, 2825 (1992); **96**, 155 (1992).

²⁷R. Alimi, R. B. Gerber, J. G. McCaffrey, H. Kunz, and N. Schwentner, *Phys. Rev. Lett.* **69**, 856 (1992).

²⁸I. Last and T. F. George, *J. Chem. Phys.* **93**, 8925 (1990); **86**, 3787 (1987); I. Last, T. F. George, M. E. Fajardo, and V. A. Apkarian, *ibid.* **87**, 5917 (1987).

²⁹Z. Li, R. Zadoyan, V. A. Apkarian, and C. C. Martens, *J. Phys. Chem.* **99**, 7453 (1995).